Surgical and Radiologic Anatomy (2019) 41:823–831
https://doi.org/10.1007/s00276-019-02235-6

ORIGINAL ARTICLE

Geometric morphometric contribution to septal deviation analysis

Thomas Radulesco[1,2] · Djamel Hazbri[1,3] · Patrick Dessi[1] · Pascal Adalian[3] · Justin Michel[1,2]

Received: 27 November 2018 / Accepted: 28 March 2019 / Published online: 2 April 2019

Abstract

Purpose The nasal septum presents inter-individual conformational variations. The objectives of this study were to establish a validated protocol for nasal septum analysis using geometric morphometrics (GM) to establish a classification of septal deviations (SD).

Methods This was a retrospective study including two groups of patients: patients operated on by septoplasty (SD group) and patients without nasal obstruction (control group). The 3D segmentation model was extracted from CT scans. Thirty landmarks were defined on the nasal septum and validated by MANOVA Procrustes. Using a clusterization process, the septum was classified to reflect its different conformations. Nasal resistances were compared between the two groups.

Results Fifty scans of patients with SD were included. The percentage of variability due to measurement error was 7.9% across all landmarks. We identified two clusters for the SD group. Using GM, conformation of cluster 1 (S-shaped) and cluster 2 (C-shaped) was visualized and identified. There was a statistically significant difference regarding nasal resistance between each cluster in the SD group compared with the control group ($p < 0.05$).

Conclusions This work is a first step in SD exploration, contributing to a clearer appreciation of the interactions between nasal conformation and function. An SD classification was devised based on a reliable and reproducible statistical analysis. Enhanced understanding of conformation/function interactions will improve the diagnosis and treatment of nasal obstruction.

Keywords Nasal septum · Nasal obstruction · Septal deviation · Geometric morphometrics · Landmarks · Cluster

Introduction

The nasal septum is a bony–cartilaginous structure separating the nasal fossae. It displays very different inter-individual conformations [8, 13, 14, 16]. It is rarely straight and may present anterior, posterior or associated deformities [21]. Any septal deviation (SD) can impede airflow and be responsible for the sensation of nasal airway obstruction (NAO) [10, 11, 23]. The prevalence of NAO is high in the general population [21] and often results in significant impairment of quality of life and sleep [2]. Surgical treatment of SD depends on the type of deviation [4], but mainly consists of septoplasty.

✉ Thomas Radulesco
thomas.radulesco@ap-hm.fr

[1] Department of Oto-Rhino-Laryngology and Head and Neck Surgery, APHM, La Conception University Hospital, 147 Bvd Baille, 13005 Marseille, France

[2] Aix Marseille Univ, CNRS, IUSTI, Marseille, France

[3] Aix Marseille Univ, CNRS, EFS, ADES, Marseille, France

Numerous attempts to classify SD have been proposed in the literature, but none has been widely adopted [1, 8, 10, 13, 14, 16, 17, 20, 23]. These experiments were based on visual clinical or endoscopic descriptions, living subjects, cadavers or on CT scan analyses. Since the late 1980s, a revolution has occurred in the techniques used to analyze anatomical structures of biological subjects [2–4]. Geometric morphometrics (GM) offers a powerful set of tools for capturing the shape of complex objects and for statistical analyses of shape variations. Shape is captured in 2 or 3D, using landmarks whose coordinates (x, y, z) serve as the database [15]. This process provides a representation of the shape of the studied object. GM is widely used in the anthropological and medical fields [18, 19]. Using GM, it is possible to compare the shape of anatomical structures and select individuals according to their shape. To date, no study has studied the nasal septum conformation by GM and landmark placement.

The objectives of this study were to determine a protocol for nasal septum analysis by means of GM, and to study pathological morphological variations of the nasal septum to establish an SD classification.

Materials and methods

Ethical considerations

All patients gave written consent for participation in the study that has been performed according to the Declaration of Helsinki, and procedures have been approved by a local ethics committee.

Population

This was a retrospective study involving patients operated on by septoplasty in our department (tertiary center) between January 2017 and January 2018.

Two groups of patients were included, an SD group and a control group.

For the SD group, inclusion criteria were:

- Age over 18 years.
- Presence of SD on endoscopic examination.
- Presence of NAO objectified by rhinomanometry (resistance of one nasal fossa greater than 0.30 sPa/mL, non-reversible after vasoconstrictor test).
- Presence in the medical file of a preoperative CT scan.

The CT scan acquisition protocols were as follows: CT scan Siemens Somatom Definition (Siemens Healthcare) or General Electric Light Speed LS 16 Pro (GE) multizone helical scanner with the following parameters: 120-Kv, 130 mAs, 0.6 mm sections every 0.3 mm.

For the SD group, exclusion criteria were:

- Age under 18 years.
- Absence of a CT scan in the patient's medical file.
- CT scans containing metal or dental artifacts.
- Absence of preoperative rhinomanometry.
- Presence of other causes of NAO (turbinal hypertrophy, nasal valve collapse, rhinitis) confirmed by rhinomanometry with vasoconstriction test.

The control group comprising healthy adult volunteers not complaining of NAO allowed us to compare nasal resistances between our clusters and a healthy population. No CT scans were performed in the control group.

Methods

All statistical analyses were performed with R® (R Core Team).

3D segmentation

Generation of the three-dimensional surface model was done using ITK-SNAP® (ITK-SNAP 3, University of Pennsylvania). Threshold values between adjacent structures were obtained using ImageJ® (v.1.44o, National Institutes of Health) using the half maximum height (HMH) method, obtained by calculating mean values over 10 gray [9] (Fig. 1).

Landmarks

According to Bookstein [2, 4], there are three types of landmarks. Type 1 landmarks are reproducible anatomical points such as suture between two bones. Type 2 landmarks are those whose position is supported by geometry (e.g., maximum curvature). Type 3 landmarks are less precise. Landmarks in the anterior two-thirds portion of the nasal septum are cartilaginous and therefore cannot belong to type 1.

A bone landmark and a mucosal landmark were positioned opposite to one another to determine the percentage of variation between bony and mucosal sites. Procustes MANOVA [12] was used to determine the percentage variation between these landmarks within the same perimeter. After determining the measurement error between these structures, it was possible to continue placing landmarks along the entire nasal septum (bony and cartilaginous portions).

Landmark positioning was done on AVIZO 7.0® (Visualization Sciences Group, Burlington, MA, USA). The *x*, *y*, *z* coordinates were then exported to R studio® (Integrated Development for R. RStudio, Inc., Boston, MA URL). Thirty landmarks were defined for each individual (Table 1). In addition to the landmarks on the septum itself, landmarks on facial bone were also used at the piriform aperture and crista galli to represent the septal "bony environment" [18]. Figure 2 shows the location of these landmarks and Table 1 specifies their definition.

Repeatability

Landmarks were positioned twice by the same operator at a 2-week interval on 20 CT scans. Landmark coordinates were compared and the percentage of variability associated with measurement error was evaluated by MANOVA Procrustes to determine repeatability [12].

Clusters

Clusterization is a statistical method designed to group individuals according to common criteria (here, the shape of the nasal septum). This clusterization was performed

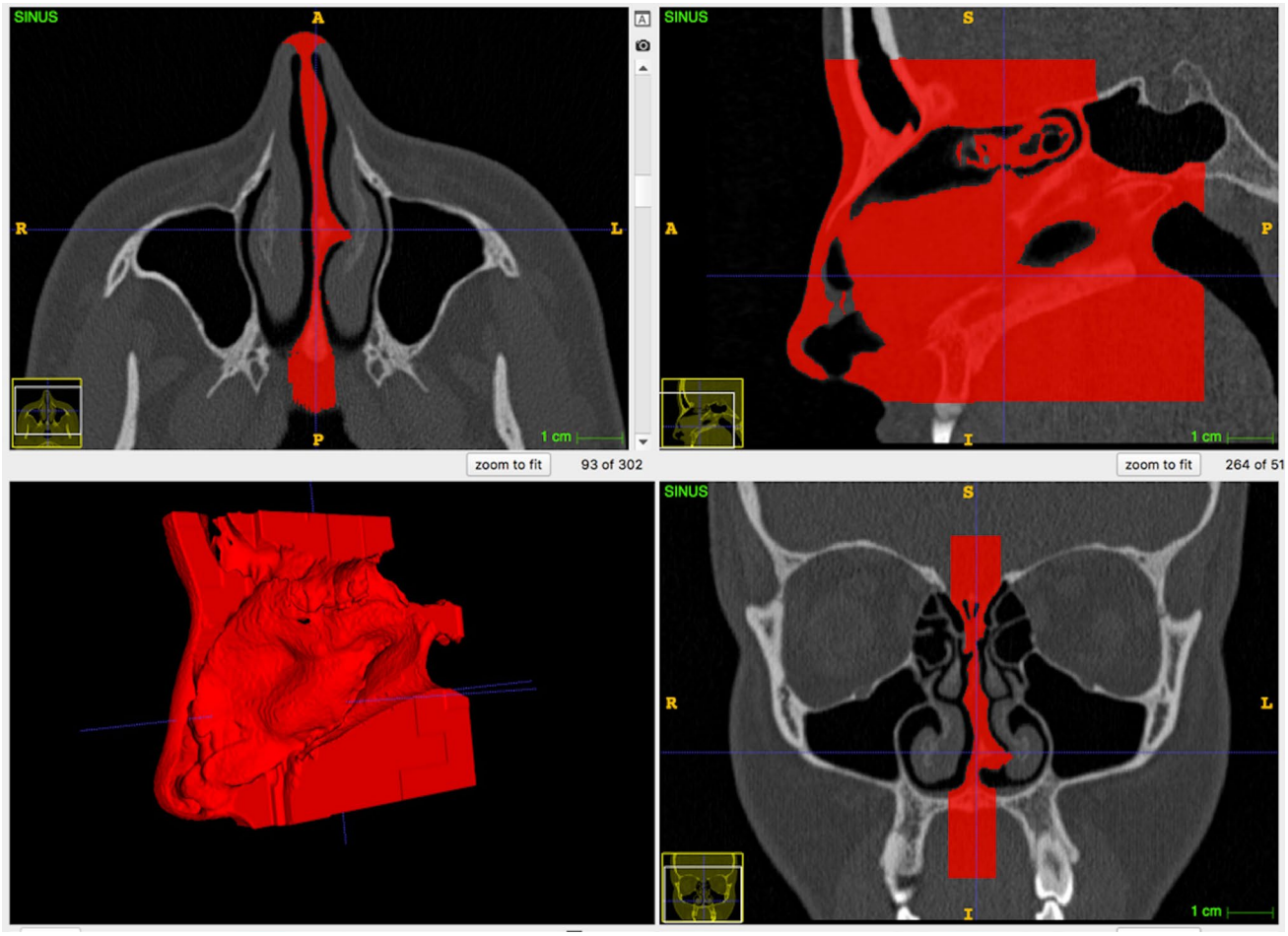

Fig. 1 3D segmentation model in an individual with SD

on the landmark coordinates of each individual. Using R studio® (HCPC function of the FactomineR package) and the raw *x*, *y*, *z* cohorts of our 30 landmarks, the pathological subjects could be classified according to Euclidean distances reflecting their conformation differences [20]. Thus, two individuals belonging to the same cluster have similar shapes, while two individuals belonging to two different clusters have different shapes.

Then, within each cluster, procrustean superimposition with principal component analysis (PCA) was performed and we defined subjects with extreme nasal septum conformations (minimum and maximum individuals along PC1). The hypothetical mean individual at the midpoint of the PCA was termed the "benchmark subject".

To validate the functional significance of our clusters, we compared the mean nasal resistance of all individuals in each cluster with the mean nasal resistance of the control group using the Wilcoxon–Mann–Whitney test.

Results

Populations

Fifty CT scans of patients having undergone septoplasty were included and anonymized (only age, sex, and rhinomanometric data were known). Mean age was 31 years (18–63). Gender distribution was 28 females (mean age: 28 years) and 22 males (mean age: 34 years) (SR = 0.78). Mean nasal resistance in this population was 2.85 sPa/mL (4.02 sPa/mL on the right and 2.84 sPa/mL on the left).

The control group comprised 30 individuals (19 females and 11 males, SR = 0.57) with a mean age of 33 years (20–56). Mean resistance was 0.58 sPa/mL (0.53 sPa/mL on the right and 0.63 sPa/mL on the left). Mean resistance was 0.48 sPa/mL (0.40 sPa/mL on the right and 0.60 sPa/mL on the left) in females and

Table 1 Number, type and definition of landmarks used during the study

Anatomical structure	Number	Type	Definition
Bone	**1**	**I**	**Sphenoidal rostrum**
Septum (left side)	2	II	Junction between the anterior part of sphenoid bone, the vomer and the posterior part of the perpendicular lamina of the ethmoid bone
Septum (left side)	3	II	Posterior extremity of the vomer
Septum (left side)	4	II	Maximum curvature for posterior septal spur
Septum (left side)	5	II	Junction point between the most anterior part of the vomer and the maxillary bone
Septum (left side)	6	II	Anterior junction point between the vomer and the perpendicular lamina of the ethmoid and the quadrangular cartilage
Septum (left side)	7	II	Point between the perpendicular lamina of the ethmoid bone and nasal bones
Septum (left side)	8	I	Anterior nasal spine
Septum (left side)	9	II	Most anterior point of quadrangular cartilage
Septum (left side)	10	II	Maximum curvature of the quadrangular cartilage
Crista galli	**11**	**I**	**Upper part of crista galli**
Septum (left side)	12	II	Maximum curvature for anterior septal spur
Piriform aperture	**13**	**I**	**The most anterior point of the nasal bone (median plane)**
Piriform aperture	**14**	**I**	**Median anterior part on the left side of the nasal bone**
Piriform aperture	**15**	**I**	**Suture zone between the left side of the nasal bone and the maxillary bone**
Piriform aperture	**16**	**II**	**Maximum lateral curvature on the left side of the piriform aperture**
Piriform aperture	**17**	**II**	**Curvature inversion zone between the lateral part of the piriform aperture and the lower part on the left side**
Piriform aperture	**27**	**I**	**Median anterolateral part of the nasal bone on the right side**
Piriform aperture	**28**	**I**	**Suture zone between the nasal bone (right side) and the maxillary bone**
Piriform aperture	**29**	**II**	**Maximum lateral curvature of the right piriform aperture**
Piriform aperture	**30**	**II**	**Curvature inversion zone between the lateral part of the piriform aperture and the lower right part**
Septum (right side)	18	II	Junction area between anterior part of the sphenoid bone, the vomer and the posterior part of the perpendicular lamina of the ethmoid bone
Septum (right side)	19	II	Posterior part of the vomer
Septum (right side)	20	II	Maximum curvature for posterior septal spur
Septum (right side)	21	II	Junction point between the most anterior part of the vomer and the maxillary bone
Septum (right side)	22	II	Anterior junction point between the vomer and the perpendicular lamina of the ethmoid bone and the quadrangular cartilage
Septum (right side)	23	II	Point between the perpendicular lamina of the ethmoid bone and nasal bones
Septum (right side)	24	II	Most anterior point of quadrangular cartilage
Septum (right side)	25	II	Maximum curvature of the quadrangular cartilage
Septum (right side)	26	II	Maximum curvature for anterior septal spur

Texts in bold are "environmental" landmarks of the face

0.77 sPa/mL (0.91 sPa/mL on the right and 0.68 sPa/mL left) in males.

There was no significant difference in age ($p = 0.74$) or gender ($p = 0.6$) between the two groups. For females, mean resistance was 3.25 sPa/mL (5.24 sPa/mL on the right and 1.79 sPa/mL on the left side). For males, mean resistance was 2.35 sPa/mL (2.48 sPa/mL on the right and 4.19 sPa/mL on the left). The difference was statistically significant ($p = 9.68\text{E} - 8$).

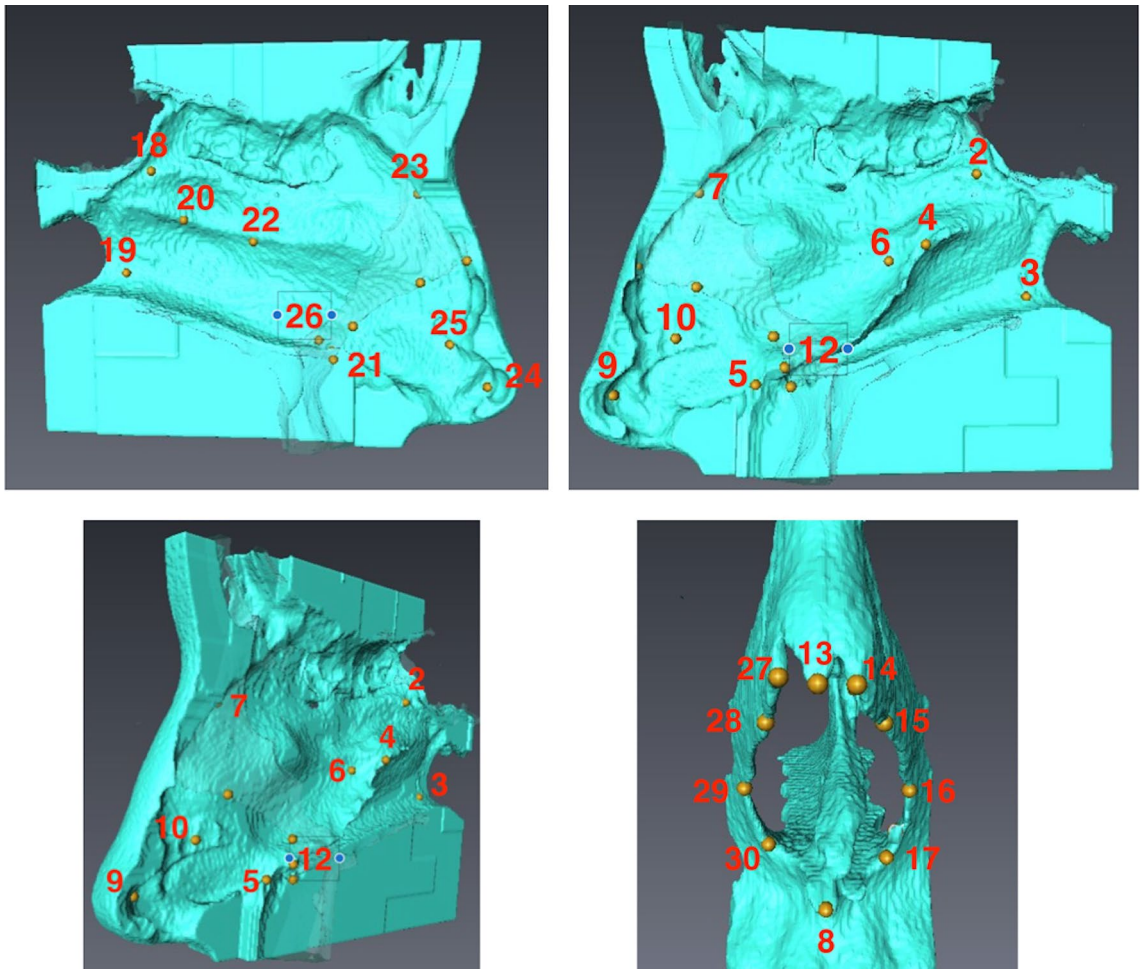

Fig. 2 Position of landmarks used on the nasal septum: right side view, left and ¾ left side; and piriform aperture

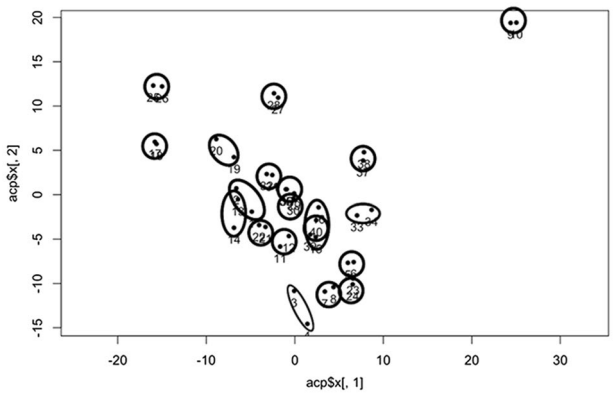

Fig. 3 Representation of repeatability along the PC1 according to the PC2. The percentage measurement error difference is 7.9%

Landmarks

Reliability

Repeatability was tested by MANOVA Procrustes. The percentage of variability due to measurement error was 7.9% across all landmarks (Fig. 3).

Clusters

We were able to identify two different clusters (Fig. 4).

In cluster 1, principal component (PC) 1 and PC2 represented, respectively, 13.3% and 11.2% of the variability. Figure 5 shows the subjects representing the maximum and minimum of variability per PC1.

In cluster 2, PC1 and PC2 represented, respectively, 21% and 15.5% of the variability.

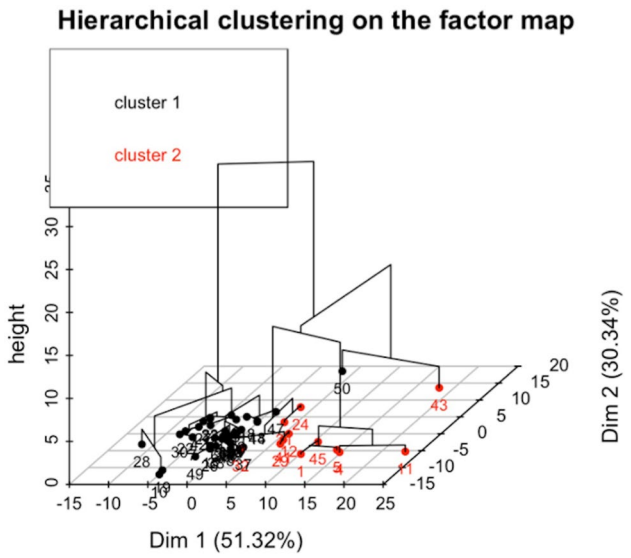

Fig. 4 Dendrogram in 3D representation. Clusters 1 and 2 are represented by different colors in projections on main component number 1 according to component number 2. This figure represents the dendrogram in three dimensions and the position of the individuals in our analysis. The dendrogram makes it possible to visualize concretely the distribution of the groups or "clusters" that we have identified. Group 1 is shown in black, group 2 in red (color figure online)

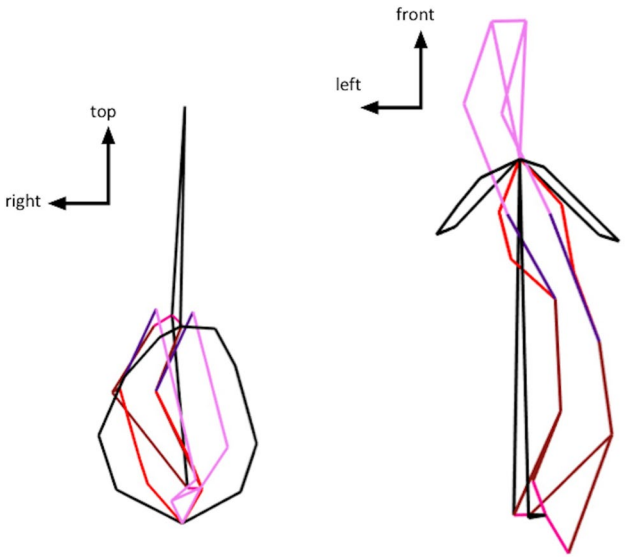

Fig. 5 Individual representation showing maximum variability depending on PC1 for cluster 1 in a front view (left) and in a top view (right)

Figure 6 shows the subjects displaying the maximum and minimum variability according to PC1.

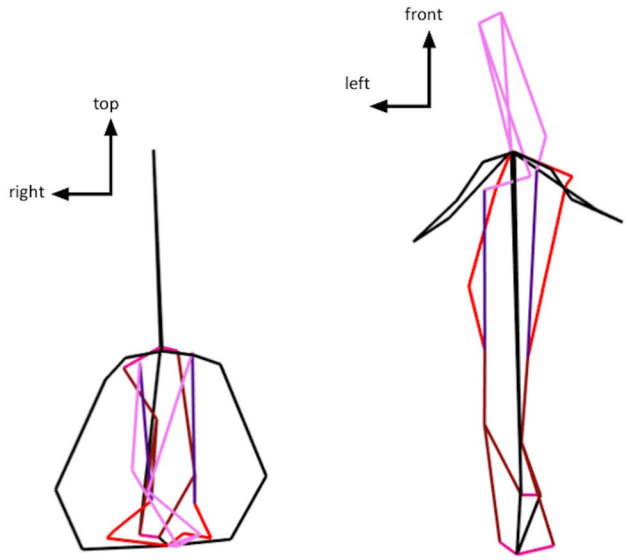

Fig. 6 Individual representation showing maximum variability depending on PC1 for cluster 2 in front view (left) and in top view (right)

Table 2 Classifications of SD in our study

	Cluster 1	Cluster 2
Axial	S-shaped deviation	C-shaped deviation
Frontal	C-shaped with posterior septal spur	C-shaped with anterior septal spur
Mean resistances	High $R = 3.01$ sPa/mL	Very high $R = 4.52$ sPa/mL

Correlation of clusters with rhinomanometric data

Cluster 1 (black) consisted of 36 individuals; the mean nasal resistance of subjects was 3.01 sPa/mL. Cluster 2 (red) consisted of 14 individuals; the mean nasal resistance of subjects was: 4.52 sPa/mL. Regarding the control group, there was a statistically significant difference between resistances in the two clusters ($p = 7.8547\text{E}-7$ and $p = 0.0006$, respectively). There was no statistically significant difference between the two clusters ($p = 0.405$).

Classification of deformations (Table 2)

We were able to establish a classification of the SD in two morphological types. Cluster 1 was characterized as S-shaped SD with bilateral nasal obstruction. Within this cluster, the closer the findings to the "benchmark subject", the fewer were the deformations we observed. The degree of deformation decreased the closer one gets to the consensual subject. The difference between the maximum and the minimum of PC1 and 2 was based on the lateralization of

the deviation. Cluster 2, which had higher resistances than cluster 1 (though not significant), was characterized by a highly deviated anterior septum in its anterior part (watch glass shaped) with a thick anterior spur. Again, within this cluster, the degree of deformation decreased the closer our observations moved toward the "benchmark subject". The difference between the maximum and minimum of PC1 and 2 was based on the lateralization of the deviation.

Discussion

Three-dimensional reconstruction from CT data is a method commonly used in medical anthropology [24]. However, defining the gray level threshold (separating soft tissue from bone and air) can be problematic. To ensure maximum precision, we applied the HMH technique to set a mathematical value for this transition zone where the change in gray levels is progressive [9]. Additional manual adjustments were made, essentially the removal of structures adjacent to the septum (turbinates, ethmoid) and included in the semi-automatic segmentation because of their proximity to the septal walls. This process provided a highly accurate three-dimensional segmentation of the desired anatomical structure.

Landmarks corresponded to anatomical loci identifiable from one individual to another among all the specimens in the study [3, 4]. No nasal septum landmarks are described in the literature. For each area of clinical interest, we defined landmarks according to the Bookstein classification. The low percentage of variation due to measurement error (7.9%) across all nasal septal landmarks is evidence of reliable and repeatable analyses.

GM focuses on studying the shape of objects in two or three dimensions. This method, originally developed for the study of non-living elements, was later applied in various fields of developmental biology and medicine. GM provides an objective analysis that is not based on the author's point of view. Indeed, the clusterization process is based exclusively on a statistical model.

Principal component (PC) analyses show the wide anatomical variability of the septum. Goergen et al. [7] used GM to study the interactions between the nasal septum and the skeleton of the facial mass in humans during growth. However, they took a pediatric 7- to 18-year-old population and the benchmarks used were located on the periphery of the septum, not the most deviated septum area. In our study, we defined and used landmarks located at the anterior section of the cartilaginous septum. These landmarks were validated by performing repeatability tests using MANOVA Procrustes. The choice of landmarks correlated with areas of clinical relevance and landmarks were located on the most deviated parts of the nasal septum: the anterior portion, the anterior spur and the posterior septal spur. These are type II landmarks located at maximum curvature level. By definition, they are less precise than type I landmarks, but the low level of differences related to measurement error (7.9%) demonstrates the good reliability of the morphological descriptions performed.

Many statistical techniques serve to separate a population into different classes or subgroups. In our study, we used clustering, a reliable and recognized method reported in the literature to identify two clusters of patients [26]. The compactness of the clusters highlights the presence of very small intra-class differences, thus reflecting good homogeneity within each group. One cluster corresponded to S-shaped deviations and the other to C-shaped deviations. In the literature, many studies have described and established SD classifications [1, 8, 10, 13, 14, 16, 17, 20, 23]. Cottle [6] ranked SD into four groups: subluxation, large spurs, caudal deflection and tension septum. Other studies were based on subjective visual findings at clinical or endoscopic examinations [10, 17]. A study published in 2012 showed that, in a population receiving septoplasty, the rate of agreement with CT scan was 71.9% for the Guyuron classification and 50% for the Mladina classification [27]. These correlation rates remain low and consequently the above-mentioned clinical classifications should not impact the surgical decision. Other more recent studies calculated their findings using computed tomographic imaging data. In 2003, Buyukertan studied nasal septum morphology, dividing it into ten segments to better characterize and locate deformities. Other authors have also used CT scan to determine levels of deviation and "stress" zones [5]. In a review of the literature, Teixeira et al. [22] established that most SD classification systems described anterior deformation (C-shaped), reverse C-shaped deviations, and S-shaped or inverted S-shaped deformations. We found the same classification in our study, since the "inverted" side corresponded to maximum or minimum depending on PC1 or PC2. The concordance with our results confirms the objectivity of Teixeira's classification, which should be preferred against all others in the literature.

All the above-mentioned studies were based on visual clinical descriptions of living, anatomical subjects or on CT scans. None of them made use of GM, which presents the advantage of being applicable to a large cohort of subjects.

The classification obtained in our study (S-shaped: cluster 1; C-shaped: cluster 2) highlighted the fact that nasal resistances differed depending on the cluster. Moreover, in cluster 1, we found that the SD was bilateral. This classification may influence the surgical procedure to be performed, as S-shaped deformations therefore require bilateral rectification of the nasal septum.

As some patients with SD may have no symptom, we compared nasal resistances within our groups. The present study also established an objective link between SD and NAO by means of rhinomanometry. Recently, Verhoeven et al. [25] reported that there was no association between the type of SD and the degree of NAO. However, this claim was based on a subjective, visual-analogical scale. In our study, nasal resistances showed a significant statistical difference between the symptomatic population and the control group. The defined clusters therefore display a clinical–functional correlation. Mean resistance in cluster 1 (= 3.01 sPa/mL) was lower than in cluster 2 ($R = 4.52$), although we did not find a statistically significant difference ($p = 0.4$). However, the number of subjects in our clusters was unequal, with 36 individuals in cluster 1 and only 14 in cluster 2. This suggests that cluster 1-type deviations are likely to be more common in the general population than cluster 2-type deviations. However, regarding nasal resistances in our population, it is important to keep in mind that we used a convenient sample of patients presenting only SD, excluding other causes of NAO. In the general population, nasal resistances may vary compared to our groups, in the presence of inferior turbinate hypertrophy or nasal valve collapse.

Our GM study enabled us to define 30 landmarks on the nasal septum. This work is a first step in the exploration of the nasal septum and represents a contribution to a better understanding of the interaction between nasal conformation and function. The correlation of septal deformities with increased nasal resistance confirms the clinical relevance of the results obtained. Finally, we were able to establish a classification of nasal septum deformities based on a reliable and reproducible statistical method. Surgical planning could be established according to the GM-derived morphological classification.

Enhanced understanding of conformation and function interactions will help improve the diagnosis and treatment of nasal obstruction. In future, computational fluid dynamics analyses could be performed on individuals presenting septal deviation and nasal obstruction.

Author contributions TR: main author. DH, PD: data collection. PA: statistics. JM: study design

Funding None.

Compliance with ethical standards

Conflict of interest The authors declare that they have no conflict of interest.

References

1. Baumann I, Baumann H (2007) A new classification of septal deviations. Rhinology 45(3):220–223
2. Bookstein F (1982) Foundations of morphometrics. Annu Rev Ecol Evol Syst 13:451–470
3. Bookstein F (1993) Morphometric tools for landmark data: geometry and biology. J Classif 10(1):133–136
4. Bookstein F (1997) Landmark methods for forms without landmarks: morphometrics of group differences in outline shape. Med Image Anal 1:225–243
5. Buyukertan M, Keklikoglu N, Kokten G (2003) A morphometric consideration of nasal septal deviations by people with paranasal complaints: a computed tomography study. Rhinology 41:21–24
6. Cottle M, Loring G, Fischer Gaynon I (1958) The maxilla–premaxilla approach to extensive nasal septum surgery. AMA Arch Otolaryngol 68:301–313
7. Goergen M, Holton N, Grünheid T (2017) Morphological interaction between the nasal septum and nasofacial skeleton during human ontogeny. J Anat 230(5):689–700
8. Grymer L, Melsen B (1989) The morphology of the nasal-septum in identical-twins. Laryngoscope 99(6):642–646
9. Guyomarc'h P, Santos F, Dutailly B, Desbarats P, Bou C, Coqueugniot H (2012) Three-dimensional computer-assisted craniometrics: a comparison of the uncertainty in measurement induced by surface reconstruction performed by two computer programs. Forensic Sci Int 219(1–3):221–227
10. Guyuron B (1999) A practical classification of septonasal deviation and an effective guide to septal surgery. Plast Reconstr Surg 104(7):2202–2210
11. Heimer D (1983) Sleep apnea syndrome treated by repair of deviated nasal septum. Chest J 84(2):184
12. Kendall DG (1984) Shape manifold, procrustean metrics and complex projective spaces. Bull Lond Math Soc 16:81–121
13. Kim J, Cho JH, Kim SW, Kim BG, Lee DC, Kim SW (2010) Anatomical variation of the nasal septum: correlation among septal components. Clin Anat 23(8):945–949
14. Krajina Z, Bumber Z (1982) Contribution to nasal-septum deformities. Acta Oto-Laryngol 93(3–4):291–294
15. Michel J, Paganelli A, Varoquaux A, Piercecchi-Marti MD, Adalian P, Leonetti G, Dessi P (2015) Determination of sex: interest of frontal sinus 3D reconstructions. J Forensic Sci 60(2):269–273
16. Miles B, Petrisor D, Kao H, Finn R, Throckmorton G (2007) Anatomical variation of the nasal septum: analysis of 57 cadaver specimens. Otolaryng Head Neck 136:362–368
17. Mladina R, Skitarelic N, Poje G, Subaric M (2015) Clinical implications of nasal septal deformities. Balk Med J 32:137–146
18. Moreddu E, Puymerail L, Michel J, Achache M, Dessi P, Adalian P (2013) Morphometric measurements and sexual dimorphism of the piriform aperture in adults. Surg Radiol Anat 35(10):917–924
19. Oxnard C, O'Higgins P (2009) Biology clearly needs morphometrics. Does morphometrics need biology? Biol Theory 4(1):84–97
20. Rao J, Kumar E, Babu K, Chowdary V, Singh J, Rangamani S (2005) Classification of nasal septal deviations—relation to sinonasal pathology. Indian J Otolaryngol 57(3):199
21. Roithmann R, Cole P, Chapnik J, Shpirer I, Hoffstein V, Zamel N (1995) Acoustic rhinometry in the evaluation of nasal obstruction. Laryngoscope 105(3):275–281
22. Teixeira J, Certal V, Chang ET, Camacho M (2016) Nasal septal deviations: a systematic review of classification systems. Plast Surg Int 2016:7089123
23. Tomasi M (1997) The deviated nose. Classification and treatment. A propos of 100 cases. Ann Otolaryngol Chir Cervicofac 114(1–2):41–50
24. Zeng W, Chen G, Ju R, Yin H, Tian W, Tang W (2018) The combined application of database and three-dimensional image registration technology in the restoration of total nose defect. J Craniofac Surg 29(5):e484–e487

25. Verhoeven S, Schmelzer B (2016) Type and severity of septal deviation are not related with the degree of subjective nasal obstruction. Rhinology 54(4):355–360
26. Ward JH (1963) Hierarchical grouping to optimize an objective function. J Am Stat Assoc 58(301):236–244
27. Wee JH (2012) Classification and prevalence of nasal septal deformity in Koreans according to two classification systems. Acta Otolaryngol 132(1):52–57